Available online at www.sciencedirect.com

ScienceDirect

Journal of the European Ceramic Society 34 (2014) 3871–3877

www.elsevier.com/locate/jeurceramsoc

Shrinkage control of yttria-stabilized zirconia during ac electric field-assisted sintering

R. Muccillo *, E.N.S. Muccillo *

Center of Science and Technology of Materials – CCTM, Energy and Nuclear Research Institute – IPEN, Travessa R 400, Cidade Universitaria, São Paulo, SP 05508-900, Brazil

Received 19 January 2014; received in revised form 10 April 2014; accepted 20 April 2014
Available online 28 May 2014

Abstract

Yttria-stabilized zirconia pellets were easily and accurately sintered to a predetermined sintering level, including near full density, in an experimental arrangement consisting of a vertical dilatometer and an ac adjustable power supply. Conventional and electric field-assisted sintering steps can be combined, starting from temperatures above 800 °C and applying 1000 Hz alternating electric fields in the range 80–160 V cm^{-1}. A systematic comparison of the microstructures and impedance diagrams of samples conventionally and electric field-assisted sintered to the same density levels shows that the non-conventional sintering method gives significantly small grains in agreement with previous observations. The results show that this sintering method can be applied to produce materials partially sintered at any desired shrinkage level.

Keywords: Sintering; Dilatometry; Impedance; Microstructure; ZrO_2

1. Introduction

Electric field-assisted sintering without application of a mechanical stress of polycrystalline ceramic materials, mostly investigated on zirconia–yttria compounds, is under intense investigation. Sintering a pre-formed ceramic body in a few seconds, with low cost equipment, is highly attractive. As the basic mechanisms responsible for this short time and low temperature sintering are not yet fully explained, it is essential to take into account the exact role of the intrinsic and extrinsic parameters, and to vary these parameters to evidence potential experimental artifacts. As intrinsic parameters we define here the applied ac with varying frequencies or dc electric fields, which may act at the interfaces or in the bulk, and the extrinsic parameters as those related to the specimen geometry and electrical conductivity, temperature, etc., which determine the power dissipation and the electric current density.

Earlier studies on tetragonal zirconia polycrystals (3YSZ) emphasized the enhanced sintering rate due to dc or ac electric field application.[1] In that case, the ac electric field was found to be more effective than a dc field to reduce the sintering temperature and the final average grain size. For yttria fully stabilized zirconia (8YSZ) a reduction of the sintering temperature needed for the densification onset was explained as a consequence of its relatively higher ionic conductivity.[2] The primary action of the ac electric field on green compacts was found to be the welding of the grains/particles.[3] Depending on the nature of the material under investigation and the experimental parameters, the result of the application of an electric field to a ceramic compact may be restricted to this stage of welding of the grains.[4]

In spite of the short sintering time for densification with application of an electric field, an impressive reduction of the sintering temperature of fully stabilized zirconia was reported when high voltages were applied.[5] The electric current density was also claimed to play an important role for the success of this method of sintering: relatively very low current densities (1 mA mm^{-2}) show no effect, i.e., do not provoke shrinkage, whereas current densities 65 times larger result in appreciable shrinkage. Moreover, the interruption of the current flow stops the shrinkage and

* Corresponding authors. Tel.: +55 11 31339203; fax: +55 11 31339276.
E-mail addresses: muccillo@usp.br (R. Muccillo), enavarro@usp.br (E.N.S. Muccillo).

http://dx.doi.org/10.1016/j.jeurceramsoc.2014.04.046
0955-2219/

sustaining the current in the electrolytic region leads to a large increase in densification kinetics.[6] Another interesting reported feature is that the densification curve shows no difference in experiments with the application of the electric field during heating up the samples or at a fixed temperature.[2] Examination of the microstructure of electric field-assisted sintered cubic stabilized zirconia evidenced a limitation of this technique. The high electric currents changed the main fracture mechanism from the intragranular to the intergranular mode in a clear demonstration of grain boundary weakening, namely, susceptible to fracture.[7]

Various recent successful attempts have also been made to demonstrate that this sintering method can be applied to several electroceramics, such as Y_2O_3-stabilized ZrO_2,[2–9] MgO-doped Al_2O_3,[10] Co_2MnO_4,[11] Gd_2O_3-doped $BaCeO_3$,[12] SiC,[13] Gd_2O_3-doped CeO_2,[14] $SrTiO_3$,[15] SnO_2,[16] and Y_2O_3.[17]

In the reported works, the main differences in the experimental approach refer to the specimen shape and the applied electric field (ac or dc). In some experiments either an electric field was applied during the sample heating or a suitable electric field was applied at a constant temperature, where the sample electrical conductivity is estimated to be sufficient to enable an electric current pulse to produce the electric field-assisted sintering. In the first case, the current pulse is triggered when a certain temperature and therefore an adequate sample electrical conductivity is reached. In the second case, when an appropriate voltage is applied and when an incubation time has elapsed.[10] Both cases have been currently reported as "flash sintering" because the elapsed time for the completion of the shrinkage lasts few seconds.

There is a continuous discussion in the scientific literature on the advantages of short-time sintering of ceramics as compared to traditional high temperature/large dwelling times. The former allows producing fine-grained ceramics, whereas in the latter grain growth is unavoidable. Sintered ceramics with small average grain size should present enhanced mechanical properties.[18] The question now, with the fairly recent electric field-assisted sintering, flash sintering, fast sintering, SHS-quick processing sintering and others, how those techniques may produce specimens with enhanced mechanical properties at relatively low temperatures and short times. There are few papers dealing with the evaluation of the mechanical properties in fast sintered ceramics.[19]

Here, the recently reported experimental facility was used to continuously control the sample shrinkage resulting from the electric current pulses.[8] Using this technique, multi-step sintering including electric current pulse sintering steps were developed, allowing for tuning the desired specimen shrinkage level. These results represent additional experimental data to contribute to understand the mechanisms responsible for the electric field-assisted sintering of electroceramics.[10,20,21]

2. Experimental procedure

All samples were prepared with the commercial powder (cubic ZrO_2:8 mol% Y_2O_3 TZ-8Y from Tosoh, Japan, hereafter 8YSZ) composed of 25 nm particles agglomerated into 75 μm spherical granules. The dried powders were pressed uniaxially under 46 MPa and then isostatically under 200 MPa. The green relative densities were approximately 50%. The cylindrical samples were about 5 mm in diameter and thickness approximately 5 mm. To improve the uniformity of the electric current distribution through the samples, their parallel surfaces were covered with chloroform-diluted platinum paint (Degussa Demetron A308).

A pc controlled vertical high temperature dilatometer (Anter model 1161, Pittsburgh, USA) was used. Even though the dilatometer may be operated under controlled oxidizing and reducing atmospheres, all the experiments were performed under static air. It can be operated up to 1600 °C with 1 μm sensitivity. This equipment allowed us to continuously monitor the sample shrinkage and to perform in situ electric field-assisted sintering experiments. Four platinum wires isolated in a 4-holes alumina capillary connected these current collectors either to the power supply or to the impedance analyzer. The dilatometer thermocouple measured the average local temperature close (∼5 mm) to the sample, which could be visualized in the pc monitor. Further details may be found elsewhere.[8]

For the electric current intensity measurement and recording, a variable (helipot) resistance was inserted in the current circuit. This equipment easily enables to continuously adjust the electric field intensity and time profiles.

The experimental sequence consists first in setting the temperature profile of the dilatometer (dwelling temperatures and time, heating and cooling rates).When the dwelling temperature is reached, the power supply is connected to the sample, and the voltage is turned on up to the occurrence of the electric current pulse and the consequent attained shrinkage level. The shrinkage behavior is continuously visualized in the digital gauge of the dilatometer. In this way, by varying the applied voltage, we can adjust the shrinkage rate and stop the densification at any level, monitoring the gauge.

The experimental procedure consisted in: (a) to produce a shrinkage level by adjusting the applied electric voltage magnitude (10–65 V), promoting the electric current pulse; (b) to stop the shrinkage advance at any pre-selected level, simply by interrupting the supplied voltage; (c) to trigger subsequent electric current pulses inducing additional shrinkages; (d) to progressively approach the full densification, avoiding a sample overheating, (and therefore limiting the grain growth); (e) to combine conventional sintering and electric field-assisted sintering steps.

Polished (16, 5, 3 and 1 μm average particle diamond paste) and thermally etched non-metalized surfaces of the electric field-assisted and conventionally sintered specimens were observed in an Inspect F50 FEI FEG-SEM microscope. Some of these polished specimens were mounted with Buehler epoxi thermoset and had the Vickers hardness evaluated in a Buehler Macro Vickers 5112 Hardness Tester with 150 N load during 15 s.

The $[-Z''(\omega) \times Z'(\omega)]$ impedance spectroscopy data, before and after the electric field-assisted sintering, were obtained with a 4192A Hewlett Packard impedance analyzer with a 362 HP controller in the 5 Hz–13 MHz frequency range $[f = (\omega/2\pi)]$ under a voltage amplitude of 200 mV and at temperatures in the oxide ion conductivity region.

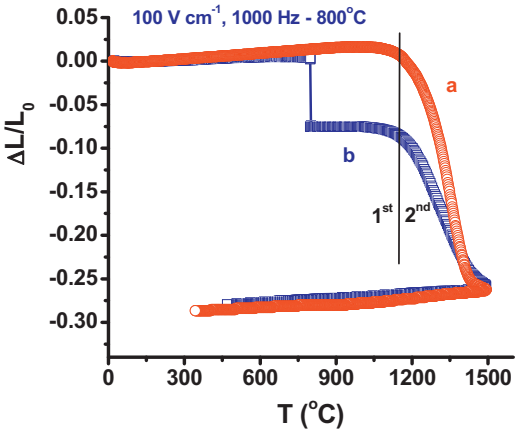

Fig. 1. Conventional and electric field-assisted sintering of ZrO_2:8 mol% Y_2O_3 green pellets. (a) Basic dilatometric curve; (b) combination of partial electric field-assisted sintering and conventional sintering. (See text for experimental details). 1st and 2nd stand for the first and the second conventional sintering stages.

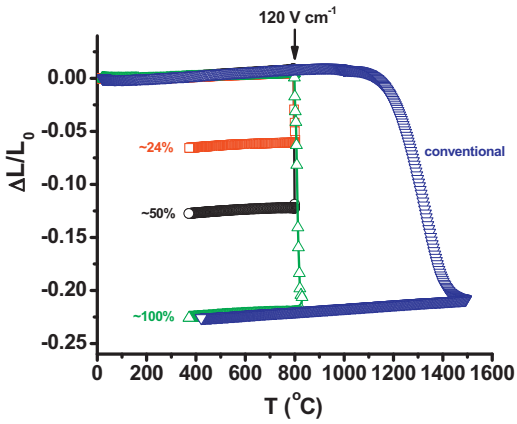

Fig. 2. Basic dilatometric curve and electric field-assisted sinterings to partial shrinkage levels. (See text for experimental details).

3. Results and discussion

3.1. Electric field-assisted dilatometry

Fig. 1 shows plots of a conventional sintering behavior up to full densification (heating rate 10 °C min^{-1}, dwelling temperature 1500 °C, dwelling time 0 min) and of a combination of a first conventional sintering step (heating rate10 °C min^{-1}, dwelling temperature 800 °C, dwelling time 30 min), followed by an electric current pulse (sintering step) triggered during the dwelling time of the previous step (100 V cm^{-1}, 5 s) and an additional conventional sintering step up to full densification (heating rate 10 °C min^{-1}, dwelling temperature 1500 °C, dwelling time 0 s).

As we already reported, in this case the main feature of the electric current pulse is to take the specimen from the 1st to the 2nd stage of sintering.[8] Even though the sample under application of electric voltage in the first sintering stage reaches the second stage of sintering (Fig. 1, curve b), it does not shrink under further heating, as expected. This means that at this stage, the defects do not have enough mobility for mass transport, known to occur in the second stage of sintering. The shrinkage proceeds only when the temperature reaches approximately 1200 °C.

Fig. 2 shows the results of dilatometric measurements on similar samples sintered according to the following procedures:

- *conventional sintering*; heating and cooling rates 10 °C min^{-1}, dwelling temperature 1500 °C, dwelling time 0 s; total shrinkage of 1.271 mm, from 5.140 mm to 3.869 mm, i.e., 24.7%); density 99% of the theoretical density (TD).
- *electric field-assisted sintering to approximately 24% of the maximum shrinkage*, (heating and cooling rates 10 °C min^{-1}, dwelling temperature 800 °C, dwelling time 30 min, initial shrinkage 0%); on the temperature plateau, at 800 °C, application of an ac field (1000 Hz) of 120 V cm^{-1} to trigger the electric current pulse; interruption of the applied electric pulses when approximately 24% of the maximum shrinkage is reached (length variation: 5.060–4.755 mm). Fig. 3a and b show the current–time and voltage–time profiles recorded during this procedure.
- electric field-assisted sintering to approximately 50% of the maximum shrinkage, same procedure up to ~50% (length variation: 5.140–4.505 mm).
- *electric field-assisted sintering to approximately 100% of the maximum shrinkage*, same procedure up to ~100% (length variation: 5.050–3.875 mm); final density 98% TD.

It should be emphasized that these experiments were repeated at least twice for each shrinkage level to assure the reproducibility of the results within the experimental accuracy of the dilatometer gauge. Negligible differences were recorded and ascribed to differences in the green microstructure, resulting from variation in the pressure of the isostatic press.

Even though the dilatometer thermocouple is not in contact with the sample, temperature variations due to the sample Joule heating were recorded at the time the electric current pulses were delivered to the sample.

As mentioned above, the important point to be emphasized here is the possibility to precisely stop the shrinkage processing at any pre-selected level, with the possibility of producing porous ceramic bodies with high skeletal density, as required, for example, for ceramic electrodes in solid oxide fuel cell devices. The selected densification is achieved by controlling the current pulse intensity and time. It may also be gradually approached by applying subsequent electric current pulses. However, the homogeneity of the porosity might depend on the thermal capacity of the sample. Fig. 3 shows the current–time and corresponding voltage–time profiles of a single pulse (Fig. 3a and b) and of two subsequent pulses (Fig. 3c and d).

The types of linear shrinkage control bring out two specific features of the electric field-assisted sintering process:

- first, in terms of shrinkage, the response time after a change in the current intensity is of the order of a second. This was already observed at the electric current trigger stage.[4] The rapid coupling between the current and the shrinkage advance, observed here, shows that it is true at any stage.

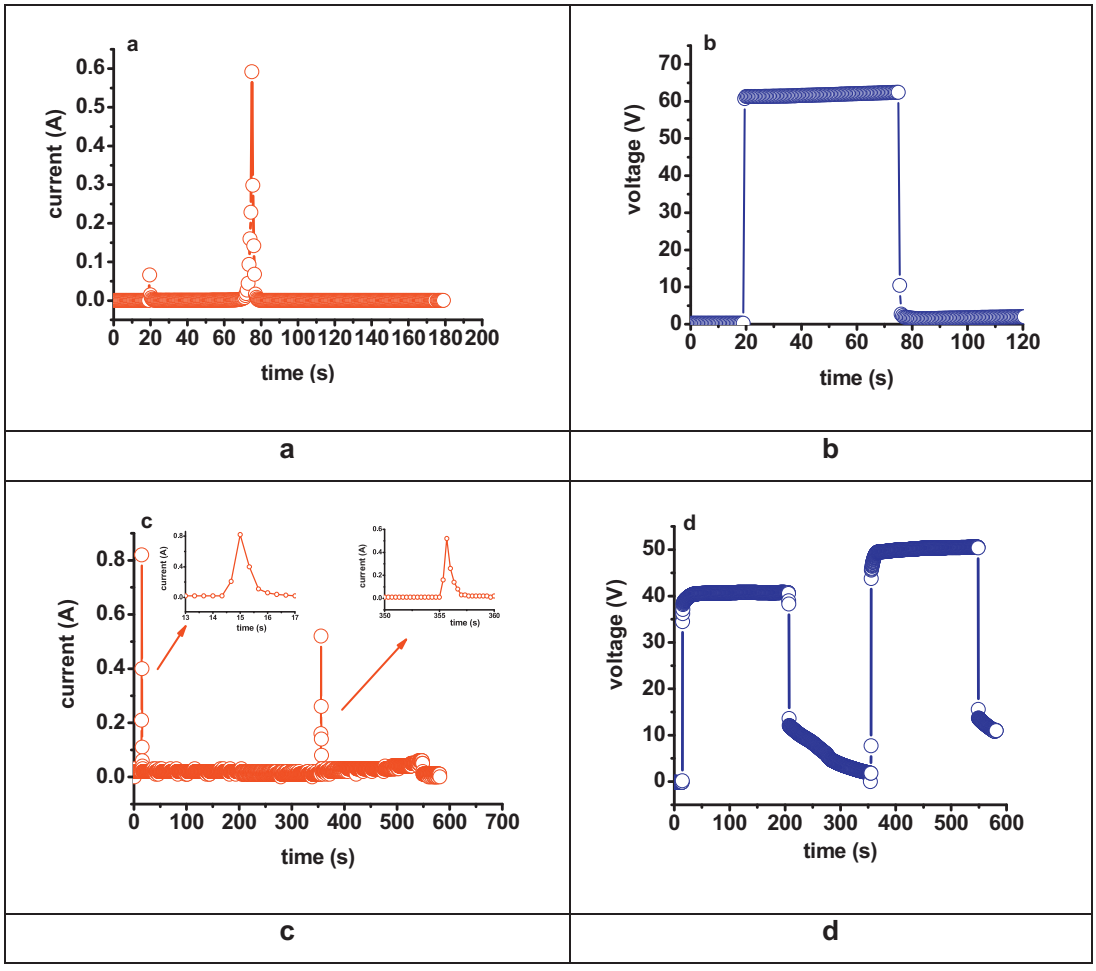

Fig. 3. Current–time (a and c) and voltage–time (b and d) profiles of typical single current pulse (top) and two successive current pulses (bottom).

- second, an electric current pulse can also be triggered through a material partially sintered. Fig. 4 shows an example of this assertion. Two similar (same mass, same uniaxial and isostatic pressings) green 8YSZ pellets were submitted to the same electric field-assisted sintering conditions (100 V cm^{-1}, 1000 Hz, 5 A limiting current) at approximately 800 °C, but one of these pellets had been pre-sintered in the dilatometer at approximately 1250 °C. Within the accuracy of the experimental setup, the shrinkage level is the same, 22%.

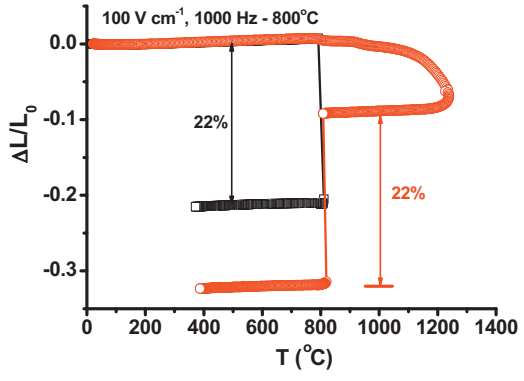

Fig. 4. Shrinkage curves of two partially electric field-assisted sintered ZrO_2:8 mol% Y_2O_3 samples. One green pellet and another pellet pre-sintered at ~1250 °C. Applied electric field: 100 V cm^{-1}; electric current limit 5 A.

3.2. Electric field-assisted sintered microstructures

The procedure here described may be used to get information on the microstructures of partially sintered materials obtained by this technique. For this purpose, pellets were sintered conventionally to the same densities as those prepared by the partial electric field-assisted sintering described above. As shown in Fig. 5, the adequate sintering temperatures, 1240 °C and 1330 °C, were simply determined on the conventional linear shrinkage of the material. For these partial conventional sintering procedures, the heating up and cooling down rates were the same.

Fig. 6 shows the shrinkage curves of the conventionally sintered samples to be compared to the partially electric field-assisted sintered samples of the same densities.

These figures show the experimental equivalence of applying an ac voltage at 800 °C and conventional sintering at higher temperatures, namely, 120 V cm^{-1} applied fields to 24%, 50%

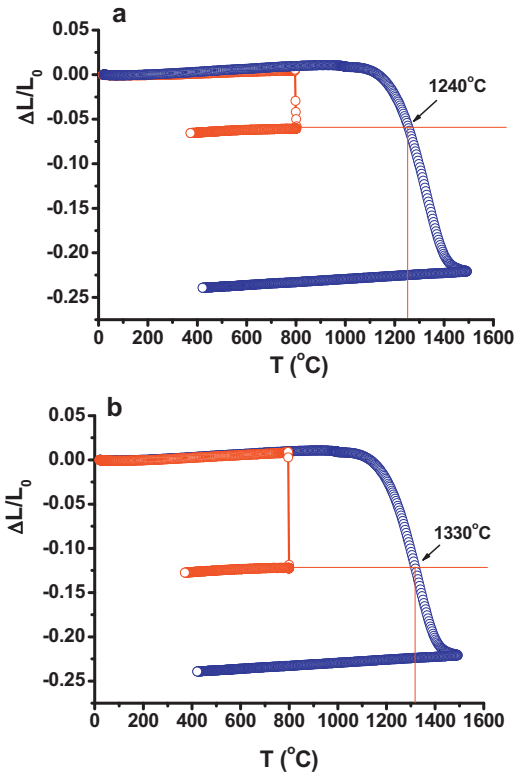

Fig. 5. Determination of the conventional sintering temperatures giving the same densities as those of the partially electric field-assisted sintered ZrO_2:8 mol% Y_2O_3 samples described above. (a) 24% and (b) 50% of maximum shrinkage.

and 100% of the maximum shrinkage is equivalent to sinter at 1240 °C, 1330 °C and 1500 °C, respectively.

Figs. 7 and 8 compare the microstructures of the electric field-assisted sintered and conventionally sintered 8YSZ green pellets, respectively. The thermal etchings were performed at 1150 °C, 1270 °C and 1400 °C for 20 min, respectively. The observations to be made are the following:

- Whatever the density level, the electric field-assisted sintered samples show sub-micron grains.
- At the same shrinkage level, the grains in the electric field-assisted sintered samples are smaller than those in conventionally sintered samples. For instance, in the "fully dense" samples, the grain sizes determined by the linear intercept method are approximately 0.8 and 2.5 μm in the electric field-assisted and in the conventionally sintered samples, respectively. This is in agreement with previous observations.
- Even at near full shrinkage the electric field-assisted sintered ceramic exhibits a residual porosity, composed of small, fairly spherical, intergranular pores. This means that the time required for the current pulse to occur and to deliver power to the whole specimen could not be enough for the pores to be eliminated.
- The partially electric field-assisted sintered materials show grains with round corners, meaning that even though the electric current pulse lasts few seconds, the temperature attained at the particle interfaces is very high.

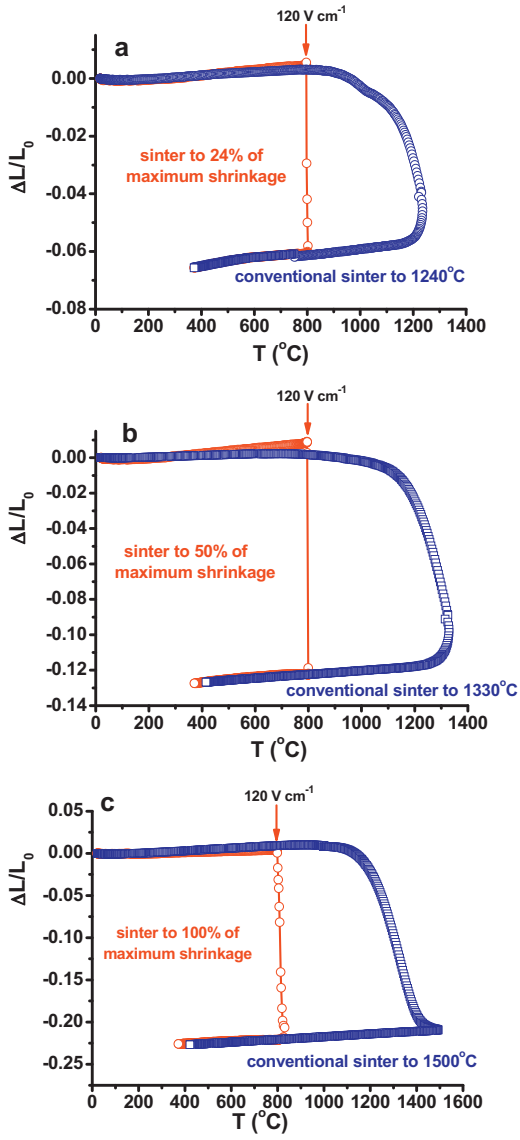

Fig. 6. Comparison of the shrinkage curves of conventionally sintered and those of partially electric field-assisted sintered ZrO_2:8 mol% Y_2O_3 samples. Electric current pulses applied to ~24% (a), ~50% (b) and ~100% (c) of the maximum shrinkage.

One should emphasize that the ac electric field-assisted sintering allows for obtaining specimens with controlled porosity and submicrometric average grain size, important steps for producing pieces with enhanced mechanical strength. The average (four indentations) Vickers hardness value of the specimen electric field-assisted shrank to 24% was 539.8 while the value for the 100% specimen was 1229.3, a value close to that of the sintered commercial YSZ (1250).[22] It is evident the larger damage (and consequently the lower fracture toughness) in the 24% sample in comparison to the 100% sample.

Impedance spectroscopy analysis was also performed at several temperatures in the 300–600 °C range on all those samples. Fig. 9 compares the $[-Z''(\omega) \times Z'(\omega)]$ impedance plots, measured at 440 °C, of the samples electric field-assisted sintered

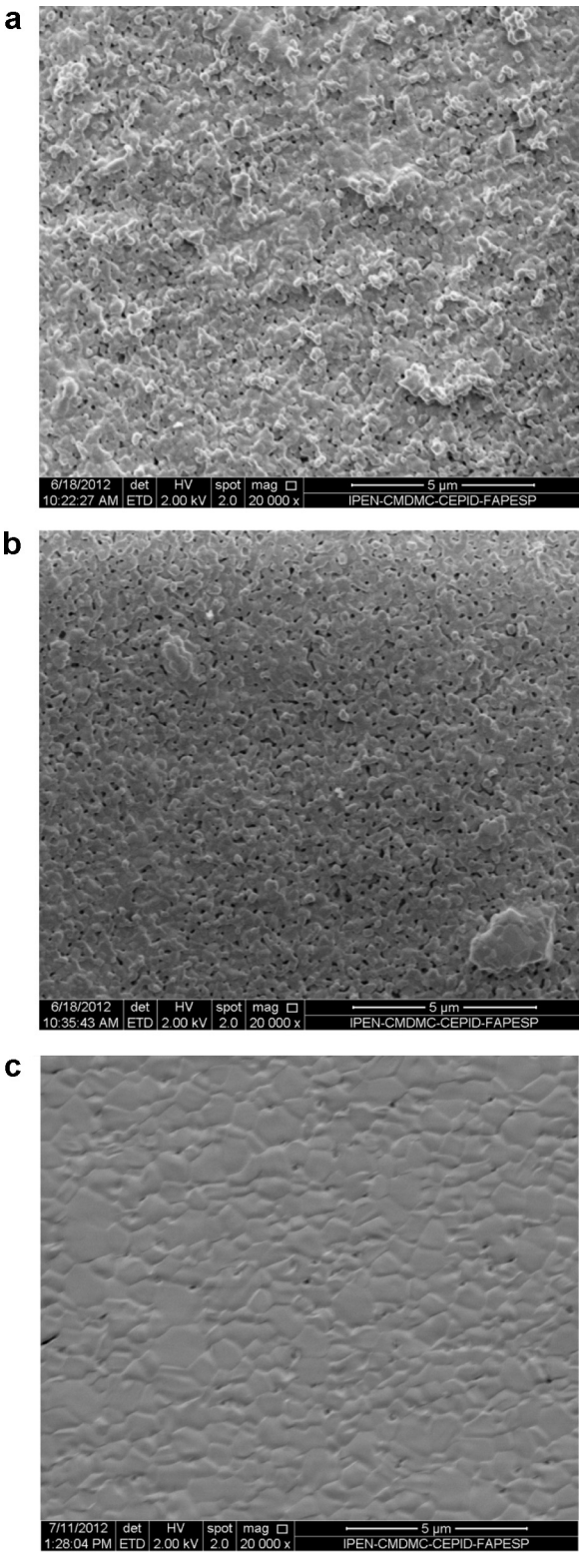

Fig. 7. Scanning electron microscopy micrographs of ZrO_2:8 mol% Y_2O_3 samples partially electric field-assisted sintered at 800 °C to ∼24% (a), ∼50% (b) and ∼100% (c) of the maximum shrinkage.

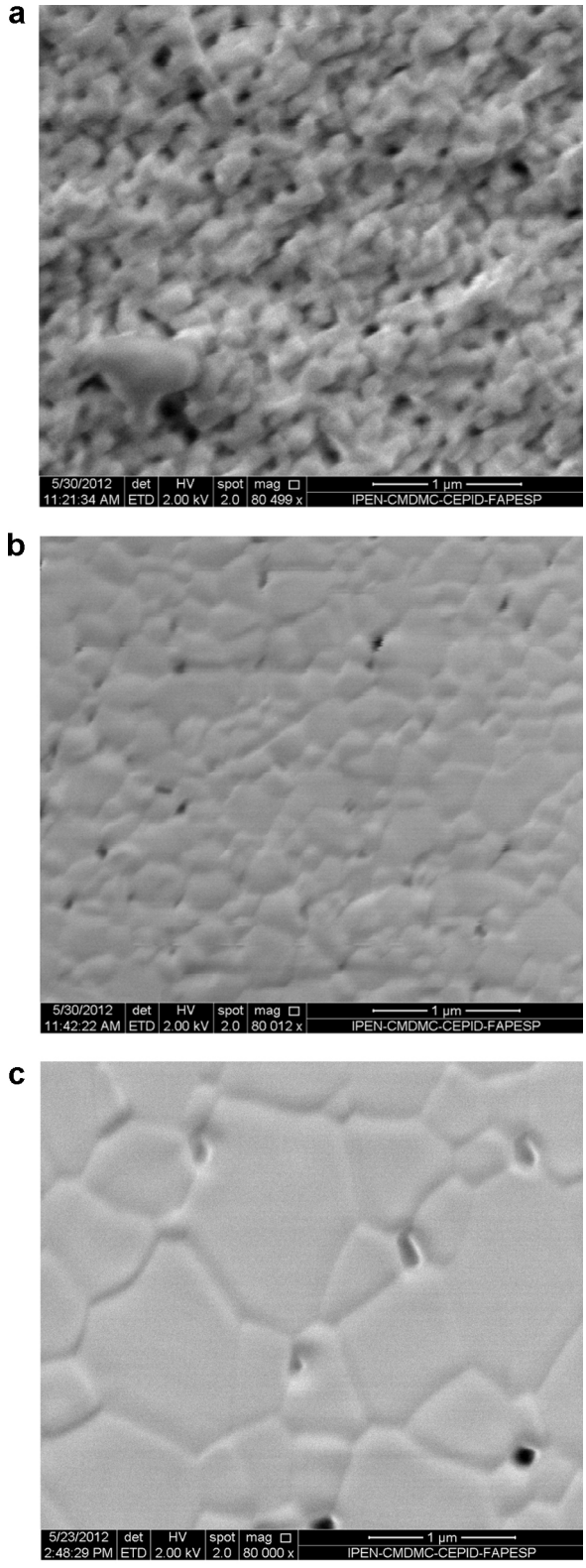

Fig. 8. Scanning electron microscopy micrographs of ZrO_2:8 mol% Y_2O_3 samples conventionally sintered at 1240 °C (a), 1330 °C (b) and 1500 °C (c).

to different shrinkage levels depicted in Fig. 2 (∼24%, ∼50% and ∼100% of the maximum shrinkage). These plots exhibit the usual two semi-circles ascribed to the electric properties of the grains and to the intergranular regions. In agreement with the SEM observations, the plots of the electric field-assisted sintered specimens show higher intergrain resistances. This is consistent with smaller grains in the electric field-assisted sintered materials.

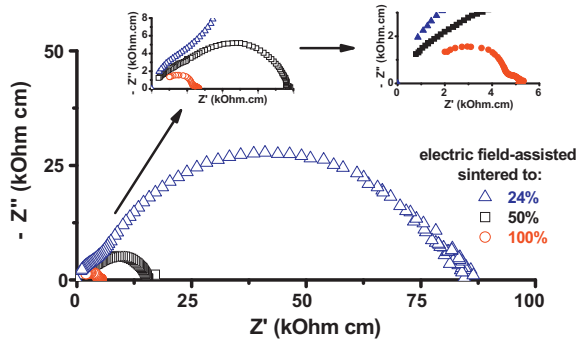

Fig. 9. Impedance spectroscopy plots of electric field-assisted ZrO_2:8 mol% Y_2O_3 samples sintered to ~24%, ~50% and ~100% of the maximum shrinkage. The insets show enlarged views of the low resistivity regions. Data collected at 440 °C.

4. Conclusions

The experimental setup using a high resolution vertical dilatometer coupled to a power supply enabled to accurately achieve pre-determined shrinkage levels of cubic yttria-stabilized zirconia green pellets upon controlled electric current pulses. It is shown that partial electric field-assisted sintering steps can be combined with conventional sintering steps. This demonstrates that the electric current pulse can be triggered through a material already partially sintered. Accordingly, subsequent electric current pulses can be implemented, for instance, to gradually approach a pre-determined shrinkage level. No evident specific feature was found in the microstructures of the electric field-assisted sintered yttria-stabilized zirconia specimens in comparison to similar specimens conventionally sintered to the same shrinkage level. The grains of electric field-assisted specimens are usually smaller and small pores appear difficult to eliminate due to the short time the electric current traverses the specimen. Moreover, the experimental setup apparently allows for producing specimens with different degrees of pore content.

Acknowledgements

To CNEN (Comissão Nacional de Energia Nuclear), CNPq (Conselho Nacional de Desenvolvimento Científico e Tecnológico) and FAPESP (Proc. 2013/07296-2) for financial support. To Dr. L.A. Genova and Y. V. França for the Vickers Hardness measurements.

References

1. Yang D, Conrad H. Enhanced sintering rate of zirconia (3Y-TZP) by application of a small AC electric field. *Scr Mater* 2010;**63**:328–31.
2. Cologna M, Prette ALG, Raj R. Flash-sintering of cubic yttria-stabilized zirconia at 750 °C for possible use in SOFC manufacturing. *J Am Ceram Soc* 2011;**94**:316–9.
3. Muccillo R, Kleitz M, Muccillo ENS. Flash grain welding in yttria stabilized zirconia. *J Eur Ceram Soc* 2011;**31**:1517–21.
4. Cordier A, Kleitz M, Steil MC. Welding of yttrium-doped zirconia granules by electric current activated sintering (ECAS): protusion formation as a possible intermediate step in the consolidation mechanism. *J Eur Ceram Soc* 2012;**32**:1473–9.
5. Downs JA, Sglavo VM. Electric field assisted sintering of cubic zirconia at 390 °C. *J Am Ceram Soc* 2013;**96**:1342–4.
6. Baraki R, Schwarz S, Guillon O. Effect of electrical field/current on sintering of fully stabilized zirconia. *J Am Ceram Soc* 2012;**95**:75–8.
7. Steil MC, Marinha D, Aman Y, Gomes JRC, Kleitz M. From conventional ac flash-sintering of YSZ to hyper-flash and double-flash. *J Eur Ceram Soc* 2013;**33**:2093–101.
8. Muccillo R, Muccillo ENS. An experimental setup for shrinkage evaluation during electric field-assisted flash sintering: application to yttria-stabilized zirconia. *J Eur Ceram Soc* 2013;**33**:515–20.
9. M'Peko J-C, Francis JSC, Raj R. Impedance spectroscopy and dielectric properties of flash versus conventionally sintered yttria-doped zirconia electroceramics viewed at the microstructural level. *J Am Ceram Soc* 2013;**96**:3760–7.
10. Cologna M, Francis JSC, Raj R. Field assisted and flash sintering of alumina and its relationship to conductivity and MgO-doping. *J Eur Ceram Soc* 2011;**31**:2827–37.
11. Prette ALG, Cologna M, Sglavo M, Raj R. Flash sintering of Co_2MnO_4 spinel for solid oxide fuel cell applications. *J Power Sources* 2011;**196**:2061–5.
12. Muccillo R, Muccillo ENS, Kleitz M. Densification and enhancement of grain boundary conductivity of gadolinium-doped barium cerate by ultra fast flash grain welding. *J Eur Ceram Soc* 2012;**33**:2311–6.
13. Zapata-Solvas E, Bonilla S, Wilshaw PR, Todd RI. Preliminary investigation of flash sintering of SiC. *J Eur Ceram Soc* 2013;**33**:2811–6.
14. Hao X, Liu Y, Wang Z, Qiao J, Sun K. A novel sintering method to obtain fully dense gadolinia doped ceria by applying a direct current. *J Power Sources* 2012;**210**:86–91.
15. Karakuscu A, Cologna M, Yarotski D, Won J, Francis JSC, Raj R, Uberuaga BP. Defect structure of flash-sintered strontium titanate. *J Am Ceram Soc* 2012;**95**:2531–6.
16. Muccillo R, Muccillo ENS. Electric field-assisted flash sintering of tin dioxide. *J Eur Ceram Soc* 2014;**34**:915–23.
17. Yoshida H, Sakka Y, Yamamoto T, Lebrun J-M, Raj R. Densification behavior and microstructural development in undoped yttria prepared by flash sintering. *J Eur Ceram Soc* 2014;**34**:991–1000.
18. Riedel R, Kleebe HJ, Schonfelder H, Aldinger F. A covalent micro/nanocomposite resistant to high temperature oxidation. *Nature* 1995;**374**:526–8.
19. Zhang J, Meng F, Todd RI, Fu Z. The nature of grain boundaries in alumina fabricated by fast sintering. *Scr Mater* 2010;**62**:658–61.
20. Raj R, Cologna M, Francis JSC. Influence of externally imposed and internally generated electrical fields on grain growth, diffusional creep, sintering and related phenomena in ceramics. *J Am Ceram Soc* 2011;**84**:1941–65.
21. Cologna M, Rashkova B, Raj R. Flash sintering of nanograin zirconia in <5 s at 850 °C. *J Am Ceram Soc* 2010;**93**:3556–9.
22. http://www.tosoh.com/our-products/advanced-materials/zirconia-powders